Thick target yield of ^{26}Al from the ^{12}C(^{16}O,x)^{26}Al$_{g.s.}$ reaction

N. P. T. Bateman,* D. W. Bardayan, Y. M. Butt, A. A. Chen, K. O. Yildiz,
B. M. Young,† and P. D. Parker
Wright Nuclear Structure Laboratory, Yale University, New Haven, Connecticut 06520-8124
(Received 1 December 1997)

Clayton and Jin have proposed that ^{26}Al in the early solar system was made by oxygen-rich cosmic rays through the ^{12}C(^{16}O,x)^{26}Al$_{g.s.}$ reaction. To test their proposal we have measured the yield of ^{26}Al$_{g.s.}$ from this reaction using the activation method. We find that the yield is too low to explain the ^{26}Al/^{27}Al ratio that has been observed in carbonaceous chondrite meteorites. [S0556-2813(98)04604-4]

PACS number(s): 26.40.+r, 26.45.+h, 25.70.Gh, 96.10.+i

I. INTRODUCTION

The Compton gamma ray telescope (COMPTEL) aboard the Gamma Ray Observatory has observed unexpectedly strong emission of gamma rays in the 3–7 MeV range from the Orion region [1]. These gamma rays are consistent with the 4.44 MeV and 6.13 MeV lines from ^{12}C and ^{16}O, although the lines are probably Doppler broadened. These observations suggest that the Orion complex is subject to irradiation by oxygen- and carbon-rich cosmic rays with energies of several MeV/nucleon.

Clayton and Jin [2] have suggested that irradiation by this type of cosmic ray might be typical of regions of massive star formation; the Orion complex is the closest region of massive star formation, and observations of the complex provide the basis for much of our knowledge of massive star formation. Since the sun is understood to have formed in a region of massive star formation, the early solar system may have been subject to irradiation by this type of cosmic ray. Clayton and Jin have proposed that these cosmic rays might be responsible for the production of many of the short-lived ($t^{1/2}<10$ Myr) radioisotopes whose daughters are found in meteorites. The standard picture of the origin of these radionuclides is that they were created in a supernova that immediately preceded, and may have caused the formation of the solar system [3]. However, as Clayton and Jin note, it is becoming increasingly difficult to accommodate all of the many short-lived species that are now known to have been present in the early solar system within this picture. In particular, shorter-lived species like ^{41}Ca($t_{1/2}=0.1$ Myr) and, especially, ^{26}Al($t_{1/2}=0.7$ Myr) put tight constraints on the formation time of the solar system; the free collapse time for one solar mass is several hundreds of thousands of years. The abundance of ^{26}Al that is believed to be typical of the early solar system [4] is 10 times higher than the abundance observed in the present day interstellar medium by COMPTEL [5]. Since Clayton and Jin's work was published, the discovery [6] of meteoritic evidence of ^{36}Cl($t_{1/2}=0.1$ Myr) has increased the problem of time scales. Clayton and Jin's proposed solution to this problem is that the short-lived isotopes were produced by the action of ''Orion type'' cosmic rays in the early solar system, so that radioisotope production could have occurred during the collapse of the protosolar cloud. Clayton and Jin focus on the production of ^{26}Al, and suggest that the most promising production mechanism for this nuclide is the ^{12}C(^{16}O,x)^{26}Al$_{g.s.}$ reaction.

The nuclear physics information that is necessary to test this proposal is the total yield of ^{26}Al$_{g.s.}$ produced when carbon or oxygen ions stop in material of solar composition. The presence of the isomeric state in ^{26}Al ($t_{1/2}=6.3$ s) complicates the situation because it cannot contribute to the ^{26}Al in the early solar system. Therefore it must be distinguished from the ground state in experiments that measure ^{26}Al production. There has been considerable work on the isotopic yield of the ^{12}C+^{16}O system; however, none of the measurements is completely relevant to the astrophysical situation that we are considering. Experiments that have measured the residual nuclei from the reaction cannot distinguish the ground state from the isomer, and experiments that have measured prompt gamma rays do not have a good absolute calibration and cannot observe the direct population of the ground state by particle decays. The previous data in the literature are shown in Fig. 1; as can be seen, there is as much as a factor of 5 variation in the measured cross sections.

To determine the astrophysically interesting yield of the ^{12}C(^{16}O,x)^{26}Al$_{g.s.}$ reaction, we have used the activation method, which involves measuring the ^{26}Al decay off line. This technique is only sensitive to the ground state of ^{26}Al, and because the beam is stopped in the target, the integration over the energy loss of the beam is accomplished automatically. As a result, it is easier to test Clayton and Jin's proposal using our data than those of previous experiments that used different techniques. In a previous paper our results were presented and their implications discussed [7], and our results have been summarized in a shorter paper [8], but the experimental details of our work have only been discussed in a dissertation [9]. This paper discusses those experimental details and our results, together with the conclusions that can be drawn from them. For a full discussion of the astrophysical consequences Ref. [7] should be consulted.

*Present address: TRIUMF, 4004 Wesbrook Mall, Vancouver, B.C., Canada V6T 2A3.
†Present address: Canberra Industries, 800 Research Parkway, Meriden, CT 06450.

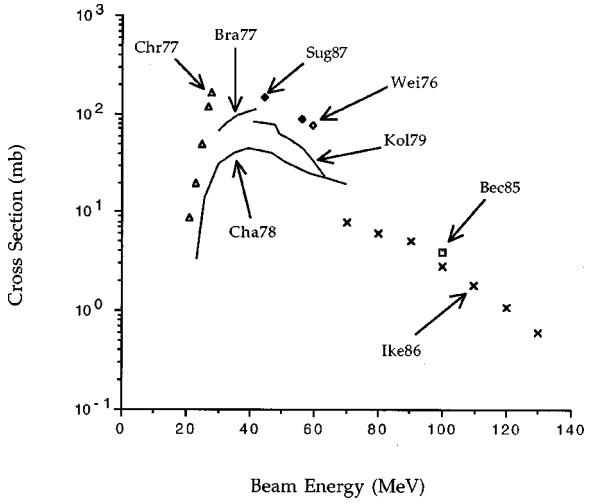

FIG. 1. Measured cross sections for the ^{12}C(^{16}O,x)^{26}Al$_{g.s.}$ reaction in the literature. Data taken from Refs. [14,16,20], and [25].

II. EXPERIMENTAL TECHNIQUE

A. Irradiation of samples

To measure the ^{12}C(^{16}O,x)^{26}Al$_{g.s.}$ yield we irradiated samples of carbon with an oxygen beam, and measured the decay of the ^{26}Al$_{g.s.}$ in these samples. Each sample was a cylinder of 99.9995% pure amorphous graphite 6 mm in diameter and 10 mm long, and the beam was incident on one end of the cylinder. The samples were of natural carbon, and so in this work when we discuss the yield of the ^{12}C(^{16}O,x)^{26}Al$_{g.s.}$ reaction we are really referring to the yield from ^{16}O+^{nat}C. The natural abundance of ^{13}C is only 1%, therefore it should not make a significant contribution to our ^{26}Al yield. Because ^{13}C was presumably present in the early solar system in natural proportions, our experiment may actually provide a better measure of the nuclear reactions in the early solar system than if we had used ^{12}C targets. Furthermore, if the cosmic rays that are bombarding Orion really come from a supernova, as has been suggested by, for example, Bykov and Bloemen [10], they should be nearly pure ^{16}O, like our beam. The dominant contaminants in our carbon samples are of much higher mass than carbon and could not make significant amounts of ^{26}Al under irradiation by the oxygen beam.

To ensure accurate charge collection, the carbon sample was placed at the end of a 15 cm long by 2 cm diameter copper tube. A ring magnet was placed around the tube to provide additional suppression of secondary electrons. Copper was chosen for its thermal properties, and because bombardment of copper by an ^{16}O beam does not readily produce ^{26}Al (or any other long-lived nuclide that can emit a γ ray of comparable energy to the ^{26}Al$_{g.s.}$ decay γ ray; see Table I). This possible background was examined by comparing the activities produced in the apparatus to those produced in a copper plate that was bombarded with the same beam. The current measured by the irradiated apparatus was compared to the current measured in a deep magnetically suppressed Faraday cup, and the readings were always consistent to within 3%. The copper tube was lined with thin foils to catch any activities that might leave the surface of the carbon sample. In the first run (at 140 MeV) a thin carbon foil (20μg cm^{-2}) was mounted inside the tube several centimeters from the carbon sample for the same reason. The beam lost a negligible amount of energy in this foil, but because it was some distance from the graphite sample, it should have remained much cooler than the sample. Despite this, the foil did not catch most of the activity; the remainder was found on the copper apparatus, closer to the sample than the carbon foil. It appears that most of the activities did not reach the carbon foil. This type of carbon foil was not used in subsequent runs.

Beams of 45, 65, and 140 MeV ^{16}O were produced by the Yale ESTU tandem. The beam spot was about 3.5 mm in diameter; so it was smaller than the samples onto which it

TABLE I. Isotopes that can produce delayed gamma lines close to 1809 keV. The arrow notation means that the parent nuclide (before the arrow) has the long half-life while the short-lived daughter nuclide (after the arrow) emits the gamma ray. ''Other lines'' refers to stronger γ-ray lines emitted by the decaying nucleus. Note that all of the decays except for that of ^{26}Al involve such lines. Data from Ref. [26].

Parent nuclide	Half-life	E_γ(keV)	I_γ	Other lines (keV)	Ratio of intensities
^{194}Au	38 h	1805.7(*6*)	0.17(*6*)	2043.7	20(*8*)
^{170}Lu	2.0 d	1809.50(*15*)	0.77(*5*)	1280.3	10.3(*9*)
				2041.9	7.7(*7*)
^{125}Sn	9.6 d	1806.701(*22*)	0.15(*4*)	1089.15	31(*12*)
				2002.1	13(*5*)
^{188}Ir→^{188}Pt	[10.2 d]	1807.8(*5*)	0.116(*23*)	2214.59	41(*5*)
		1810.2(*4*)	0.34(*4*)		
^{56}Co	77 d	1810.772(*17*)	0.657(*10*)	846.771	152.2(*51*)
				2598.459	25.8(*4*)
^{26}Al	7.4×10^5 yr	1808.63(*6*)	99.73(*8*)		

TABLE II. Details of the irradiation of the carbon samples.

Beam energy (MeV)	Charge state	Total charge (mC)	Power (W)
45	5+	200	14
65	6+	593	16
140	7+	357	30

impinged. The beam was tuned with the sample removed from the beam, so that all of the irradiation of the samples was at the full beam current, thereby keeping the temperature of the sample constant throughout each run. Beam currents of 1.5μA (charge) were used in all three measurements. The beam was integrated continuously throughout each run. Run summaries are shown in Table II. Because of the very long half-life of ^{26}Al, runs of up to 100 h were required to produce a measureable amount of ^{26}Al. The power delivered to the carbon sample was as much as 30 W; so some of the more volatile materials were lost from the carbon sample. However, aluminum is quite refractory and, as will be discussed, in all runs most of the ^{26}Al stayed in the sample.

B. Counting apparatus

The ^{26}Al$_{g.s.}$ produced in the irradiation was measured by observing the 1809-keV β-delayed gamma ray from its decay. Although 99.7% of all ^{26}Al$_{g.s.}$ decays emit this gamma ray [11], because the half-life of ^{26}Al$_{g.s.}$ is so long, its intensity was still very low and a sensitive gamma detection setup was required. We used a 25% HPGe detector with BGO Compton suppression. At 1.8 MeV the background was dominated by cosmic rays, and not by Compton-scattered photons, but the Compton shield was also an effective cosmic-ray veto, vetoing 79$\pm$2% of cosmic rays. Additional reduction in the room background was achieved by surrounding the detector (and sample) with two layers of 5-cm-thick lead bricks. Care was taken to ensure that gaps in the two layers did not overlap. ''Older'' lead bricks were used to avoid the neutron capture product ^{124}Sn which was seen in bricks that had recently been exposed to neutrons. All of the bricks were also checked for the presence of ^{207}Bi, which could also contribute to the background. The BGO shield was found to contain a considerable activity of ^{207}Bi, but because this ^{207}Bi decayed inside the shield, it was largely (88.6$\pm$1.8%) self-vetoing.

To reduce pileup, the signals from the amplifier were sent to an EG&G ORTEC 675 germanium resolution enhancer. Because the detector had not suffered significant neutron damage and the count rate was low, this unit did not significantly improve the resolution (which was 2.8 keV at 1.3 MeV in the final setup), but it did improve the pileup rejection. The γ-ray spectra were collected and stored on a PC-based MCA system. The dead time was checked with a 1 Hz pulser. The pulser period was checked against the PC clock and was found to be consistent within 0.1%. The analog-to-digital converter (ADC) dead time induced by the pulser was 55μs per pulse, which gave rise to an additional (unmeasured) dead time of about 0.006%.

The background spectrum was measured three times, once before any samples were measured, once between sample measurements, and once after all sample measurements were complete. Each sample measurement was several weeks long. No change in the background was observed between the three measurements. The weighted mean of all three background measurements was used to determine the background at the ^{26}Al$_{g.s.}$ γ-ray energy. The background spectrum measured in the middle of the experiment is shown in Fig. 2, and the observed isotopes are listed in Table III. None of the contaminant lines made a significant contribution to the gamma-ray background at 1809 keV.

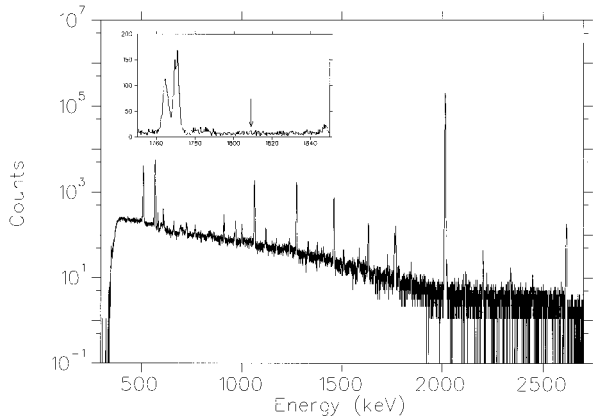

FIG. 2. Background spectrum. The region around 1809 keV is shown in the inset; the arrow marks 1809 keV. The peak at 2000 keV is from the pulser.

The carbon samples were mounted on a 1-cm-thick aluminum plate to ensure that the counting position was reproducible. This distance was chosen because 511 keV gamma rays from ^{26}Al$_{g.s.}$ decay can trigger the Compton veto. Tests with a ^{22}Na source showed that the detection efficiency was essentially constant for all distances within 3 cm of the face of the Compton shield, when the veto probability was taken

TABLE III. Observed gamma ray lines in the background spectra. The observed lines are tabulated by mass. ''e^+'' refers to annihilation radiation, and lines labeled ''(s)'' are sum peaks. Most of the observed isotopes are usual room backgrounds. The sources of the other lines are discussed in Ref. [9].

Isotope	Energies (keV)
e^+	511.0
^{7}Be	477.6
^{22}Na	1274.5
^{40}K	1460.8
^{60}Co	1173.2,1332.5
^{65}Zn	1115.5
^{108}Ag^m	614.3,722.9
^{137}Cs	661.7
^{207}Bi	569.7,1063.7,1633.4(s),1770.2,2339.9(s)
^{208}Tl	583.2,860.6,2614.6
^{209}Po	896.6
^{212}Bi	727.3
^{214}Pb	351.9
^{214}Bi	609.3,768.356,1120.3,1155.2,1238.1,1377.7
	1661.3,1729.6,1764.5,1847.1, 2118.6,2204.2,2447.9
^{228}Ac	911.2,964.8,969.0,1588.2
^{234}Pa^m	766.4,1001.0

into account. When mounted on the plate the end of the carbon sample was 2.5 cm from the shield and about 9 cm from the germanium crystal. The samples were covered with several mm of epoxy to stop the positrons in the source region. The range of positrons at the β end point is 4 mm, and when the shape of the (second forbidden) decay curve is taken into account, very few of the positrons annihilated at any significant distance from the source.

The absolute efficiency was determined with calibrated sources of ^{22}Na, ^{56}Co, ^{58}Co, ^{60}Co, ^{88}Y, and ^{152}Eu. Because all of these sources (except ^{58}Co) emit coincident γ rays in cascades which can lead to spurious vetos in the BGO shield, the calibration was performed with the veto disabled. Corrections were applied in the standard way to account for coincident sum peaks. The calibration was performed at four different times, once before the measurements, twice between runs, and once after all the measurements, though not all of the sources were used each time. Because the various carbon samples had slightly different lengths, a small correction was made, under the assumption that the activity was concentrated in the end of the sample that had been irradiated. The logarithm of the efficiency was fit to a quadratic in the logarithm of the energy over various ranges of energies to find the efficiency at 1809 keV. The variation between the different fits was generally larger than the statistical uncertainty in any one of them; this variation was treated as a systematic uncertainty. The γ-ray detection efficiency at 1809 keV found with this procedure was $1.05 \pm .05 \times 10^{-3}$.

Since this efficiency was measured with the veto disabled, to use it we also had to measure the probability that a coincident gamma ray from the ^{26}Al$_{g.s.}$ decay would veto the 1.8 MeV gamma ray. These coincident gamma rays are a 1129 keV deexcitation gamma ray and the two 511 keV gamma rays from the positron decay. These veto probabilities were measured with ^{60}Co and with ^{22}Na and ^{58}Co sources, respectively. Details can be found in Ref. [9].

C. Secondary activities

After irradiation, the samples were allowed to decay for several days before they were handled. As a result our measurements are not sensitive to short-lived activities. When the samples were removed from the target chamber the various parts of the irradiation apparatus were each placed at a distance of about 12 cm from the germanium detector to determine the distribution of the various activities throughout the irradiation apparatus. The apparatus consisted of the following.

The carbon sample: the cylinder of graphite that was bombarded by the oxygen beam.

The copper base: the piece of copper in which the carbon sample was mounted during the irradiation.

The copper tube: the 15 cm copper tube that was used for beam integration.

The lining foil: the copper tube was lined with copper foil to catch the activities that were emitted from the carbon. In the 140 MeV run (the first one) the tube was lined with tantalum foil instead of copper. We discovered that very little activity ended up on this foil, instead it ended up in the tube underneath the foil. Consequently, in subsequent runs we used a copper lining foil.

The carbon foil (140 MeV run only): as noted above, in the 140 MeV run a carbon foil was mounted across the copper tube. The beam passed through this foil, but the activities that left the carbon sample presumably did not.

Our goals in determining the location of the various activities in the apparatus were twofold; first, we needed to measure how much ^{26}Al (if any) had left the sample and to correct our yield accordingly; second, we had to deal with the the problem of beam halo. Any beam halo that extended beyond the carbon sample would hit the copper apparatus, and we needed to make two corrections for this effect. Because this beam did not hit the carbon, it should be subtracted from the integrated beam current, and if this beam halo produced any ^{26}Al in the rest of the apparatus, this fact needed to be taken into account. We chose copper in part to minimize this last problem, and our measurements of the activities produced by bombarding copper samples show that it was not a concern.

A variety of activities were found on different parts of the apparatus. ^{7}Be was seen in the 65 and 140 MeV runs. At 65 MeV it was only found in the carbon sample, whereas at 140 MeV only 76% of the ^{7}Be activity remained in the carbon sample. ^{22}Na and ^{24}Na were observed in all runs with distributions that were identical; furthermore, if the activity that remained in the carbon is neglected, the distribution of the ^{7}Be was identical to that of the sodium isotopes. We deduce that all three of these isotopes were produced in the carbon samples, and that different elements were ejected from the carbon with different efficiencies. The activities that were found on the copper, and used to determine the total beam current that had hit the copper apparatus, were ^{77}Br and a line at 835 keV that results from the decay of mass 72 isotopes.

These results show that material was ejected from the carbon samples at all of the energies. A key question in interpreting what happened to the ^{26}Al that was produced in the carbon is whether the material was boiled off because of the high temperature, or was sputtered off by the incident beam. Our results strongly suggest that the material was evaporated rather than sputtered. ^{22}Na and ^{24}Na are made by quite different processes in the carbon, therefore their depth distribution in the carbon sample should be different. However, their chemistry is identical; so the fact that their distributions were identical in the 65 and the 140 MeV runs implies that sodium atoms (and presumably other atoms as well) were mobile within the carbon matrix. In earlier runs with more tightly focused beams, visible marks were observed in a piece of carbon which had been sputtered. The material around the carbon was also blackened by the sputtered material. In the runs reported here none of the samples was visibly marked, and the copper base and foils were not discolored. Finally in the 140 MeV run 76% of the ^{7}Be was retained in the carbon sample, while only 0.3% of the sodium stayed in the carbon. This is not consistent with any realistic picture of sputtering. The fact that so little of the sodium stayed in the sample was actually to our advantage, and influenced our choice of amorphous graphite as the target material. In an earlier run we had used a glassy carbon target, which had much better thermal properties than the

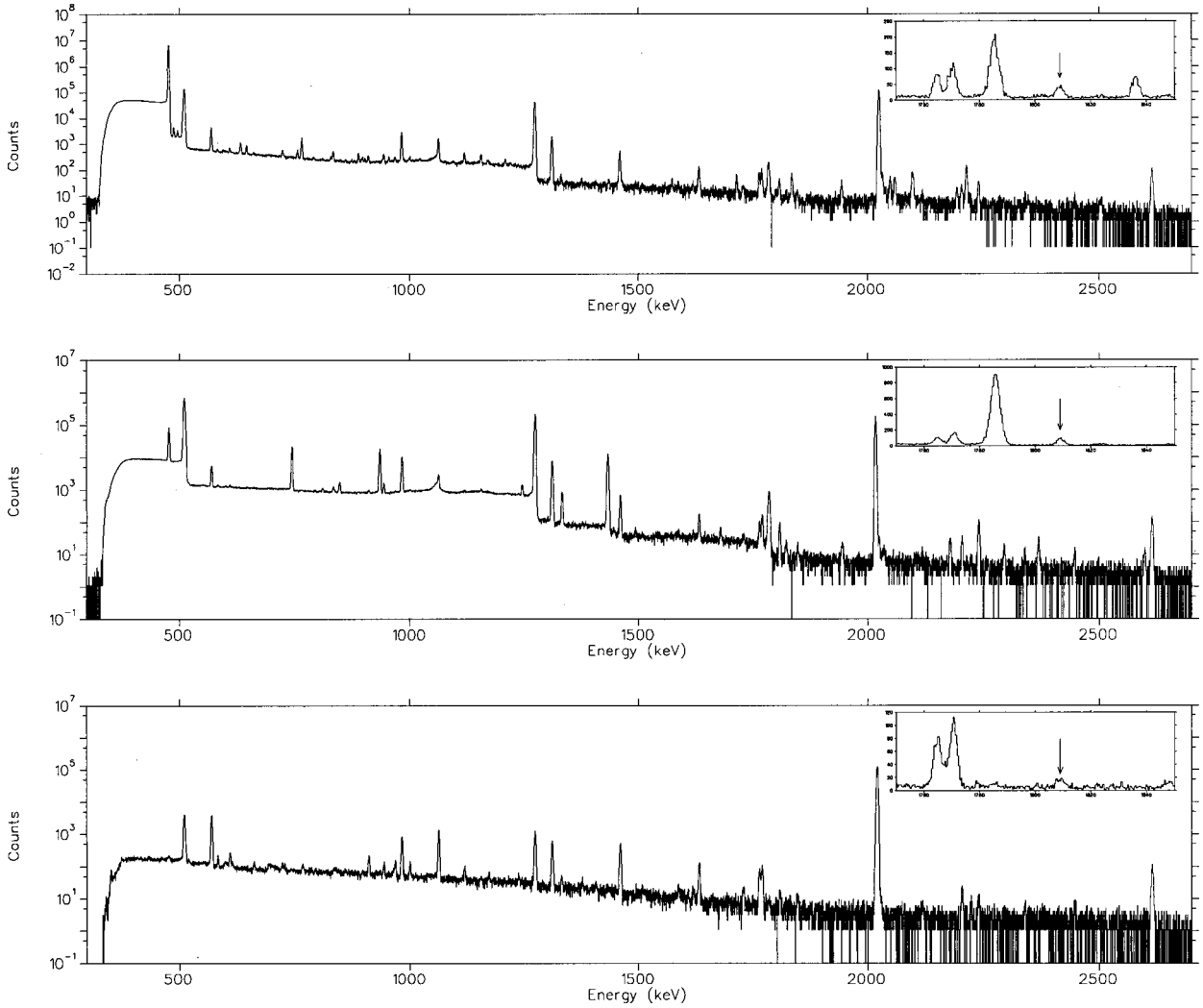

FIG. 3. Spectra of the carbon samples irradiated at 140, 65, and 45 MeV (from top to bottom, respectively). The region around 1809 keV is shown in each inset; the arrows mark 1809 keV.

amorphous graphite, and almost all of the ^{22}Na was retained in the carbon. The background from the pileup of the 1.27 MeV γ ray made it impossible to see the ^{26}Al line. So, in effect, we heated the target with the beam to the point at which ^{22}Na and ^{26}Al were physically separated.

Because of these facts, we conclude that the emission of different radioisotopes from the carbon target depended upon the thermal properties of the respective elements. Sodium is, of course, much more volatile than beryllium or aluminum; so it is reasonable to assume that the distribution of ^{26}Al is much more similar to the ^{7}Be than to that of the sodium isotopes. Although the fractions of ^{7}Be and of the sodium isotopes leaving the graphite target were quite different, of the materials external to the graphite target, the *relative* distributions of ^{7}Be and of the sodium isotopes were essentially the same, indicating that it was reasonable to assume the same relative distribution for the ^{26}Al which had left the target.

The arguments for our assumptions about the distribution of ^{26}Al in each run are as follows: for both the 45 and 65 MeV runs a large portion of the sodium was retained in the carbon, and in the 65 MeV run all of the ^{7}Be stayed in the carbon. Furthermore, we measured the amount of ^{26}Al in the lining foil (which contained most of the evaporated sodium) for both these runs, and found no ^{26}Al. Therefore, we believe that no ^{26}Al left the carbon in either of these runs, though we used the measured quantity of ^{26}Al in the lining foils, and the distribution of the sodium isotopes, as a limit for the amount of ^{26}Al that had left the carbon sample in each of these runs. For the 140 MeV run 24% of the ^{7}Be left the carbon foil. In this case we assume that the ^{26}Al that left the carbon had the same distribution on the apparatus as the ^{7}Be, the ^{22}Na, and the ^{24}Na. It seems likely that these distributions were simply detemined by geometrical factors which are identical for all isotopes. $32\pm3\%$ of the activity that was not in the carbon ended up in the carbon foil that was placed across the copper pipe. We measured the amount of ^{26}Al in this foil to determine how much ^{26}Al had left the carbon sample.

D. Chemical separation of ^{26}Al

Because of the pileup of two 1.27 MeV γ rays from ^{22}Na, it was not possible to count the ^{26}Al in the carbon foil from

TABLE IV. The observed beam-induced gamma-ray lines. Those marked with an ''(*s*)'' represent sum peaks. Escape peaks have not been listed here. Not all of the lines of any particular isotope were observed at each energy. Details on the origins of the various isotopes can be found in the text and in Ref. [9].

Origin of Isotopes	Isotopes	Beam energies (MeV)	Energies (keV)
Carbon samples	^{7}Be	45,65,140	477.6
	^{22}Na	45,65,140	1274.5,1785.5(*s*)
	^{26}Al	45,65,140	1808.6
Copper apparatus	^{72}Se→^{72}As	140	834.0
	^{74}As	140	595.8
Collimators	^{88}Y	140	898.0,1836.1
	^{95}Zr	140	724.2,756.7
	^{95}Zr→^{95}Nb	140	765.8
	^{182}Re	140	1076.2,1221.4
	^{184}Re	140	792.1,903.3
	^{185}Os	140	874.8
	^{188}Ir→^{188}Pt	140	633.0/634.9,829.4,1209.8,1435.4, 1574.5, 1715.7,1802.2,1944.1,2049.8,2059.7,2096.9, 2193.67,2214.59,2347.9,2504.9
''Iron group''	^{44}Sc	65,140	1157.0
	^{46}Sc	140	889.3
	^{48}V	45,65,140	944.1,983.5,1312.1,1494.5(*s*),2240.4(*s*)
	^{52}Mn	65	744.2,848.2,935.5,1246.3,1333.6,1434.1,1945.1(*s*)
	^{58}Co	140	810.8

the 140 MeV run without first separating the ^{26}Al from the ^{22}Na. This separation was done chemically, by dissolving and precipitating the material in the foil. Aluminum does not have any other isotopes that are longer lived than a few minutes; therefore we could not add such an isotope as a tracer, to measure the efficiency of the chemical processes. However, for the chemistry that we used, beryllium behaves in the same way as aluminum; so the ^{7}Be that was already present in the carbon foil was used to trace the aluminum throughout the following process.

(1) The carbon foil was removed from its (copper) frame by dripping concentrated sulfuric acid on it. The acid was allowed to drip into a beaker. The beaker was filled to 5 ml of concentrated sulfuric acid, and 50 mg of aluminum nitrate was added as a carrier. At this point the beaker contained 45% of the ^{22}Na that was initially in the foil, and 58 $\pm$23% of the initial ^{7}Be.

(2) The acid was heated to about 180 °C, at which point the carbon evolved as carbon dioxide, and the solution became cloudy.

(3) After the acid had cooled it was diluted to 40 ml, and then neutralized with ammonium hydroxide. At a *p*H of about 4 the suspension went into solution, and as the acid was neutralized the aluminum (and beryllium) was precipitated as the hydroxide.

(4) After the precipitate had settled, 85% of the solution was drawn out of the beaker. Although care was taken not to remove the precipitate, this procedure resulted in the loss of 28 ± 4% of the remaining ^{7}Be activity.

(5) The remaining solution was passed through filter paper. After the filter paper had dried it was folded into a tight wad, and covered with epoxy to stabilize it. 6.5 ± 2.7% of the remaining ^{7}Be was lost in this step.

36 ± 8% of the ^{7}Be which had been present in the foil before the chemical separation was present in the filter paper at the end of the last step. The ^{26}Al retention was assumed to be the same as that of the ^{7}Be. The corresponding retention for the ^{22}Na was 0.18 ± 0.03%, a factor of 200 smaller. The ^{26}Al activity in the filter paper was counted; the resulting measured activity was multiplied by a factor of 2.8 ± 0.6 to take account of the activity lost in the separation and by an additional factor of 2.1 ± 0.1 to include the ^{26}Al on the copper base, as measured by its ^{7}Be activity. The resulting ^{26}Al activity was then added to the activity measured in the

TABLE V. Fitted energies and areas of ^{26}Al peaks. In method I the peak positions and energies were allowed to vary; in method II both were fixed by calibration with background lines.

Sample	Energy (keV)	Counts method I	Counts method II
Carbon 45 MeV	1809.05 ± 0.30	125 ± 21	104 ± 13
Carbon 65 MeV	1809.10 ± 0.08	713 ± 29	718 ± 29
Carbon 140 MeV	1808.89 ± 0.57	318 ± 31	311 ± 21

TABLE VI. The measured yields of $^{26}Al_{g.s.}$ for ^{16}O ions stopped in carbon. Yield is defined as the number of product nuclei produced by one incident beam nucleus. Note that the results are slightly diffferent from those in Ref. [9] because some later data are included here.

Beam energy (MeV)	Yield ($\times 10^{-5}$)
45	1.86 ± 0.39
65	4.35 ± 0.36
140	6.83 ± 0.94

graphite target, to determine the total ^{26}Al production. (The ^{26}Al remaining in the carbon corresponded to $69 \pm 10\%$ of the total.)

E. Data analysis

Each of the off-line counting runs took several weeks. Counting was stopped daily so that we could measure any drift in the amplifier and ADC gains. Each 24 h spectrum had several peaks with sufficient statistics to allow the drift to be corrected. After this correction was applied the individual spectra were summed. The final spectra were analyzed using the program GELIFIT [12], and all peaks were fit in the usual way. The spectra from the three carbon samples are shown in Fig 3. Table IV lists all of the lines that were observed in any of the three spectra and their identities. Other than the isotopes that were produced in the carbon and copper, we observed activities that can be roughly categorized as those that came from the Ta beam collimators and from the small Nb impurities in those collimators (i.e., Y, Zr, Nb, Re, Os, Ir, and Pt) and a variety of iron group nuclei (i.e., Co, V, Mn, and Sc) whose origin is less clear.

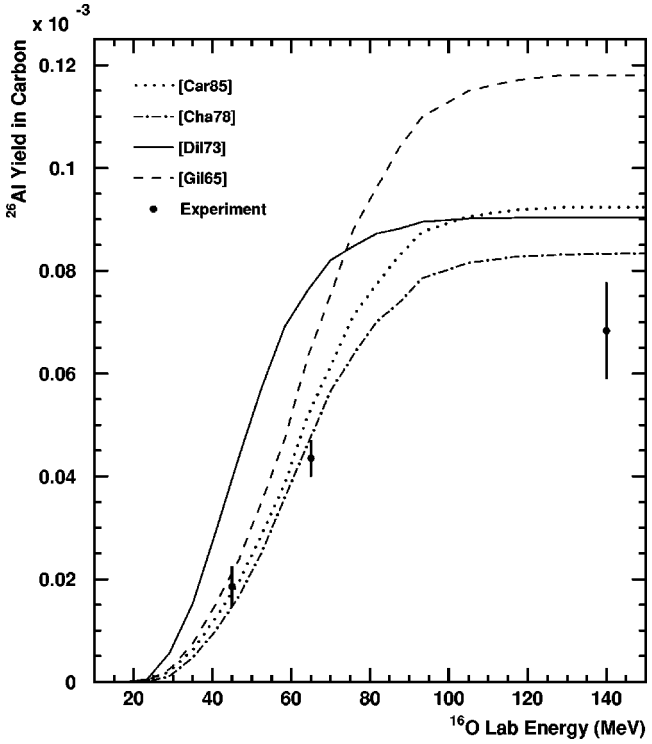

FIG. 4. Measured yields for the $^{12}C(^{16}O,x)^{26}Al_{g.s.}$ reaction. The data points are our measured results, while the curves show the results of our CASCADE calculations using different parameter sets [19,20,17] and [18]. There are no free parameters in these calculations. On the basis of these results we have chosen to use the parameters of Chan *et al.* [20] to represent our results.

The large number of identified lines in each spectrum meant that the energy calibration of each one could be established internally. For all spectra the best fit was found with a cubic or fourth order fit. The fitted energy of the ''$^{26}Al_{g.s.}$ peak'' for each spectrum is shown in Table V. In each case the measured energy is in good agreement with the energy of the $^{26}Al_{g.s.}$ line which is 1808.63 ± 0.06 keV [11]. The area of the $^{26}Al_{g.s.}$ peak was found with the peak energy and width fixed, and also with both the width and the centroid allowed to vary. The results are also shown in Table V. As can be seen the two methods give essentially the same result. In all spectra except those of the carbon samples (i.e., measurements of the foils and the filter paper, and background spectra), the statistics in the $^{26}Al_{g.s.}$ peak were too low to allow the width and energy to vary; so only the second method was used for these spectra.

To verify that the γ ray that was observed was from $^{26}Al_{g.s.}$ decay we have conducted a search of the NNDC data base for other isotopes that might produce a γ ray with an energy within 3 keV of 1809 keV and with a half-life that is longer than 1 day. Because of the length of the counting runs, any isotopes that had half-lives shorter than this would have decayed away over the course of the runs. The results of this search are shown in Table I. All of the possible contaminant lines have other much stronger lines associated with them. Two of these isotopes were in fact observed in our data, and the sum of the number of counts was corrected accordingly. Only the ^{188}Ir in the 140 MeV sample made a significant difference, and this was a 10% correction.

The total number of counts observed in a given run (after the background has been subtracted) is given by

$$N = n\,\mathrm{BR}(1809)\,\lambda\,\eta\,\frac{N_{26}^{v}}{N_{26}^{nv}}\,t, \tag{1}$$

where n is the number of $^{26}Al_{g.s.}$ atoms in the sample, BR(1809) is the probability that a $^{26}Al_{g.s.}$ decay leads to emission of an 1809 keV γ ray (99.7%), λ is the decay rate of $^{26}Al_{g.s.}$, η is the measured efficiency at 1809 keV, N_{26}^{v}/N_{26}^{nv} is the probability that the BGO veto was triggered in a given event, and t is the counting time of the run.

The total amount of ^{26}Al is then given by the sum of the ^{26}Al found in the carbon sample and the amount that had left the sample. This number was then divided by the integrated beam current to give the total yield at the three energies, which is to say the number of ^{26}Al atoms produced for each ^{16}O ion stopped in the carbon. The measured yields are shown in Table VI, and plotted in Fig. 4.

F. Theoretical calculations

The thick target yield can be found from the energy-dependant cross section $\sigma(\varepsilon)$ by

$$Y(E) = \int_0^E \frac{\sigma(\varepsilon)}{(d\varepsilon/dx)(\varepsilon)}\,\frac{N_A}{A}\,n_t\,d\varepsilon, \tag{2}$$

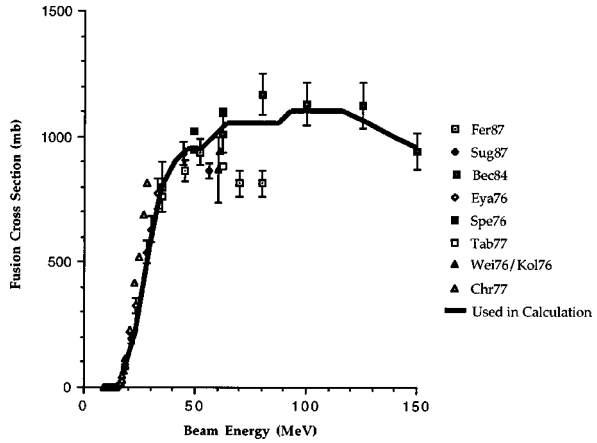

FIG. 5. Fusion cross section used in our CASCADE calculations. The data represent various measurements in the literature [15,16]. The line is the excitation function that we have used.

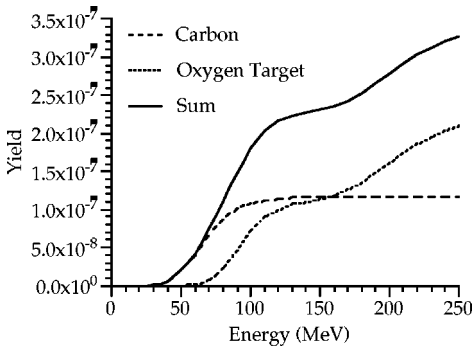

FIG. 6. Astrophysical yield of the ^{12}C(^{16}O,x)^{26}Al$_{g.s.}$ reaction (based on our measurement) and of the ^{16}O(^{16}O,x)^{26}Al reaction (based on CASCADE calculations). For ^{16}O particles incident on material of solar composition all other targets nuclides can be neglected.

where E is the beam energy, $d\varepsilon/dx$ is the stopping power, N_A is Avagadro's number, A is the molecular mass of the target, and n_t is the number of target atoms per target molecule.

To try to understand the form of our measured yields and to try to interpret it in terms of the yield of ^{26}Al$_{g.s.}$ that would be produced by oxygen cosmic rays in the early solar system, we used the Hauser-Feshbach code CASCADE [13] to calculate the excitation function for the ^{12}C(^{16}O,x)^{26}Al$_{g.s.}$ reaction. Most of the parameters used were those that Sugimitsu *et al.* [14] used to fit their data on ^{12}C+^{16}O fusion-evaporation reactions. The fusion cross sections were taken from a variety of experimental data [14–16], and these data and the cross sections that we used are shown in Fig. 5. Four different sets of data were used for the pairing energies and level densities of the relevant nuclides. These were the default values in CASCADE (from Dilg *et al.* [17]), the values from the compilation of Gilbert and Cameron [18], and the values that Carlin-Filho *et al.* [19] and Chan *et al.* [20] fit to their respective experimental data sets. These are the only parameter sets in the literature that are reasonably complete, and even the parameter set from Ref. [19] had to be supplemented by some of the data of Ref. [18].

Equation (2) was used to find the integrated yield from the cross sections calculated by CASCADE. The resulting yield curves are shown in Fig. 4 and compared to our experimental results. The curve calculated using the parameters of Chan *et al.* shows the best agreement with the data; so we have used this curve to represent the shape of the yield curve in our interpretation of our results. Note that we do not claim that our data demonstrate that our calculation has produced an accurate excitation function for the ^{12}C(^{16}O,x)^{26}Al$_{g.s.}$ reaction or that they show that the data set of Chan *et al.* is the appropriate one. Rather, because our data are consistent with the curve calculated using the parameters of Chan *et al.*, we use this curve as a template to determine the yield of ^{26}Al$_{g.s.}$ in the protosolar cloud.

III. DISCUSSION

We used Eq. (2) and the calculated excitation function for the ^{12}C(^{16}O,x)^{26}Al$_{g.s.}$reaction to find the yield of ^{26}Al$_{g.s.}$for cosmic rays stopped in the protosolar cloud (i.e., in material of solar composition). The stopping powers were calculated using TRIM [21]. This code can calculate stopping powers for mixtures of up to four elements; so the solar abundances of hydrogen, helium, and oxygen were used, and the fourth element was taken to be the average of all other elements (the solar composition of Anders and Grevasse [22] was used). As the stopping is dominated by hydrogen and helium, this is a reasonable assumption. The yield curve is shown in Fig. 6.

We have also considered the role of other target elements in the protosolar cloud; it is certainly not true that when a beam of ^{16}O is stopped in material of solar composition only the ^{12}C(^{16}O,x)^{26}Al$_{g.s.}$ reaction can contribute to ^{26}Al$_{g.s.}$ production. In particular, the ^{16}O(^{16}O,x)^{26}Al$_{g.s.}$ reaction should be important, as oxygen is twice as abundant as carbon in the solar system. Although we are in the process of measuring the yield from the ^{16}O+^{16}O reaction, for the purposes of the current discussion we use a calculated excitation function to characterize this reaction. This calculation was performed using the same parameters and the same procedure that was used for the ^{12}C(^{16}O,x)^{26}Al$_{g.s.}$ yield. The resulting yield curve is shown in Fig. 6. Other target elements are probably too rare to be important.

An upper limit on the total fluence of oxygen cosmic rays in the protosolar cloud is given by the total amount of oxygen in the solar system. Therefore, for the picture of Clayton and Jin [2] to be plausible the abundance ratio of ^{26}Al/^{16}O must be smaller than the yield of ^{26}Al$_{g.s.}$ averaged over the ^{16}O energy spectrum. Meteoritic evidence gives a standard value of ^{26}Al/^{27}Al$=5\times10^{-5}$ [4]. This can be combined with the ratio of ^{27}Al/^{16}O in the solar system [22] to give ^{26}Al/^{16}O$=2\times10^{-7}$. Note that from Fig. 6 this is within a factor of 2 of the total yield of ^{26}Al$_{g.s.}$ from oxygen-rich cosmic rays at the very highest energies. The oxygen energies cannot be any higher than 140 MeV without producing more ^{6}Li than is found in the solar system (see Refs. [7] and [23] for details of this argument). If we use our yields to estimate the fluence of oxygen in the early solar sytem, we would require that fully one-half of all the oxygen present in the solar system was injected as cosmic rays. Admittedly there are large uncertainties in our calculation, but to suggest that even as little as 1% of the oxygen presently in the solar system must have been injected into the solar system over

the short period of time available (recall that the half-life of ^{26}Al is only 0.7 Myr) at MeV-scale energies is implausible at best.

Therefore, we find that the yield of ^{26}Al when oxygen is stopped in material of solar composition is simply too small to account for the abundance of ^{26}Al in the early solar system. Other scenarios for the production of ^{26}Al by heavy-ion cosmic rays were discussed in the previous paper, and none is really plausible [7]. The problem of the origin of the extinct activities in the early solar system is thus still with us, and it appears that these activities must have come from some sort of external explosive event. The solution might lie in a scenario like that of Cameron *et al.* [24] in which the radioactive products of such an explosion are accelerated to high energies and then stopped in the protosolar cloud.

ACKNOWLEDGMENTS

We wish to thank R. Naumann for discussions about the nuclear chemistry in this experiment and A.E. Champagne for many helpful discussions. This work was supported under DOE Grant No. DE-FG02-91ER-40609.

[1] H. Bloemen *et al.*, Astron. Astrophys. **281**, L5 (1994); Astrophys. J. **475**, L25 (1997).
[2] D. D. Clayton and L. Jin, Astrophys. J. **451**, 681 (1995).
[3] A. G. W. Cameron and J. W. Truran, Icarus **30**, 447 (1977).
[4] G. J. Wasserburg, in *Protostars and Planets II*, edited by D. C. Black and M. S. Matthews (University of Arizona Press, Tucson, 1985), p. 703.
[5] R. Diehl *et al.*, Astron. Astrophys. **298**, 445 (1995).
[6] S. V. S. Murty, J. N. Goswami, and Yu. A. Shukolyukov, Astrophys. J. **475**, L65 (1997).
[7] N. P. T. Bateman, P. D. Parker, and A. E. Champagne, Astrophys. J. **472**, L119 (1996).
[8] N. P. T. Bateman, D. W. Bardayan, Y. M. Butt, A. A. Chen, K. O. Yildiz, B. M. Young, P. D. Parker, and A. E. Champagne, Nucl. Phys. **A621**, 60c (1997).
[9] N. P. T. Bateman, Ph.D. Thesis, Yale University, 1996.
[10] A. Bykov and H. Bloemen, Astron. Astrophys. **283**, L1 (1994).
[11] P. M. Endt, Nucl. Phys. **A521**, 1 (1990).
[12] D. C. Radford and R. W. Macleod, AECL computer code GELIFIT.
[13] F. Pülhofer, Nucl. Phys. **A280**, 267 (1977).
[14] T. Sugimitsu, H. Inoue, H. Fujita, N. Kato, K. Kimura, T. Tachikawa, K. Anai, Y. Ikeda, and Y. Nakajima, Nucl. Phys. **A464**, 415 (1987).
[15] P. R. Christensen, Z. E. Switkowski, and R. A. Dayras, Nucl. Phys. **A280**, 189 (1977); Y. Eyal, M. Beckerman, R. Chechik, Z. Fraenkel, and H. Stocker, Phys. Rev. C **13**, 1527 (1976); B. Fernandez, C. Gaarde, J. S. Larsen, S. Pontoppidan, and F. Videbæk, Nucl. Phys. **A306**, 259 (1978); P. Sperr, S. Vigdor, Y. Eisen, W. Henning, D. G. Kovar, T. R. Ophel, and B. Zeidman, Phys. Rev. Lett. **36**, 405 (1976); S. L. Tabor, Y. Eisen, D. G. Kovar, and Z. Vager, Phys. Rev. C **16**, 673 (1977).
[16] C. Beck, F. Haas, R. M. Freeman, B. Heusch, J. P. Coffin, G. Guillaume, F. Rami, and P. Wagner, Nucl. Phys. **A442**, 320 (1985); A. Weidinger, F. Busch, G. Gaul, W. Trautmann, and W. Zipper, *ibid.* **A263**, 511 (1976).
[17] W. Dilg, W. Schantl, H. Vonach, and M. Uhl, Nucl. Phys. **A217**, 269 (1973).
[18] A. Gilbert and A. G. W. Cameron, Can. J. Phys. **43**, 1446 (1965).
[19] N. Carlin Filho, M. M. Coimbra, J. C. Acquadro, R. Ligouri Neto, E. M. Szanto, E. Ferrelly-Pessoa, and A. Szanto de Toledo, Phys. Rev. C **31**, 152 (1985).
[20] Y.-D. Chan, H. Bohn, R. Vandenbosch, K. G. Bernhardt, J. G. Cramer, R. Sielemann, and L. Green, Nucl. Phys. **A303**, 500 (1978).
[21] J. F. Ziegler and J. Biersack, computer code TRIM91.
[22] E. Anders and N. Grevasse, Geochim. Cosmochim. Acta **53**, 197 (1989).
[23] R. Ramaty, B. Kozlovsky, and R. E. Lingenfelter, Astrophys. J. **456**, 525 (1995).
[24] A. G. W. Cameron, P. Höflich, P. C. Myers, and D. D. Clayton, Astrophys. J. **447**, L53 (1995).
[25] D. Branford, B. N. Nagorcka, and J. O. Newton, J. Phys. G **3**, 1565 (1977); H. Ikezoe, N. Shikazono, Y. Tomita, K. Ideno, Y. Sugiyama, E. Takekoshi, T. Tachikawa, and T. Nomura, Nucl. Phys. **A456**, 298 (1986); J. J. Kolata, R. M. Freeman, F. Haas, B. Heusch, and A. Gallman, Phys. Lett. **65B**, 333 (1976); Phys. Rev. C **19**, 408 (1979).
[26] National Nuclear Data Center at Brookhaven National Laboratory.